Published in final edited form as:
J Environ Monit. 2012 October 26; 14(10): 2772–2779. doi:10.1039/c2em30405h.

Size dependent aqueous dispersibility of carboxylated multiwall carbon nanotubes

Susana Addo Ntim[a], **Ornthida Sae-Khow**[a], **Chintal Desai**[a], **Frank A. Witzmann**[b], and **Somenath Mitra**[a,*]

[a]Department of Chemistry and Environmental Science, New Jersey Institute of Technology, Newark, New Jersey 07102, USA

[b]Department of Cellular & Integrative Physiology, Indiana University School of Medicine, Biotechnology Research & Training Center, Indianapolis, IN 46202, USA

Abstract

The size dependent colloidal behavior of aqueous dispersions of carboxylated multiwall carbon nanotubes (c-MWCNTs) is presented. The presence of carboxylic groups provided electrostatic stabilization in water, where the size affected agglomeration. While aspect ratio did not show any definite correlation, the hydrophobicity indices (HI), zeta potential and aggregation kinetics showed dependence on the length of the c-MWCNTs where the shorter c-MWCNTs showed significantly lower HI values, smaller particle aggregates, higher zeta potential values and higher critical coagulation concentrations (ccc) in the presence of electrolytes. Although the diameter of the short c-MWCNTs did not appear to influence their aggregation behavior, the longer c-MWCNTs showed a dependence on diameter where stability decreased with increasing CNT diameter.

1. Introduction

Carbon nanotubes (CNTs) possess some highly desirable properties, which make them attractive for a variety of applications, and their demand is expected to increase significantly over the next decade. Typically, the CNTs are chemically stable, highly hydrophobic, and rather inert in their physico-chemical interactions. Some level of functionalization is required prior to their utilization in many real-world applications that range from polymer composites to drug delivery. Functionalization also allows further conjugation with other molecules. Some of these functionalized forms are also water dispersible. Examples include surfactant based functionalization, non-covalent wrapping of the tubes with polymers,[1] (poly)peptides,[2] proteins,[3] and nucleic acids,[4] and covalent functionalization where the CNTs are chemically oxidized in the presence of strong acids.[5–8]

As CNTs find their way into industrial and consumer products, they may be inadvertently released into the environment during their production, use and disposal. While there exists the possibility for raw, unrefined, and hydrophobic CNTs to settle out of aqueous media into solid phases such as river sediments, water dispersible forms may persist in water resources increasing the risk to public health. Therefore there is a need to develop a comprehensive understanding of the fate and transport of the dispersible CNTs in aqueous media.

mitra@njit.edu; Fax: +1 973 596 3586; Tel: +1 973 596 5611.

The colloidal behavior of CNT dispersions is important in understanding their behavior in the aquatic environment, and there are several reports in the literature addressing this issue.[9,10] Time-resolved dynamic light scattering (TRDLS), Raman spectroscopy, zeta-potential measurements, and UV-Visible spectroscopy have been used to investigate the aggregation kinetics of CNTs.[11,12] Precipitation of the carboxylated CNTs under the influence of different salts has shown that[12,13] precipitation is dependent on the charge on the cations, and in general these nanoparticles have followed the well-established Derjaguin–Landau–Verwey–Overbeek (DLVO) theory.[14,15]

Several toxicological studies have investigated the effect of size on the toxicity of particles comparing nanometer and micrometer particles of the same composition. Metal oxides such as CuO and TiO_2,[16] gold,[17] monodispersed amorphous spherical silica[18] as well as SiO_2 nanoparticles[19] have shown size dependent cytotoxicity. In all these studies, the particles were observed to be more toxic in the smaller size ranges than the larger ones, except TiO_2 which showed the opposite effect. The literature on the size dependent behavior of CNTs at this present time is scanty at best. It is important to realize that CNTs represent a diverse group of nanotubes that vary in size, shape and chirality. For example, in recent years there has been growing interest in shorter CNTs for high field quasiballistic electron transport,[20] hydrogen storage,[21] and energy storage systems such as in lithium batteries.[22] Since size alters many of the properties of CNTs, it may also affect its fate and transport and is an important parameter when CNTs are in consideration as pollutants. The objective of this paper is to investigate the effects of size and aspect ratio on the colloidal stability of carboxylated multiwall carbon nanotubes (c-MWCNTs) in electrolytic environments.

2. Experimental

2.1 Chemicals

Multiwall carbon nanotubes of different sizes were purchased from Cheap Tubes Inc. These are shown in Table 1 with their lengths, outer diameters (OD) and aspect ratios, and are referred to as $MWCNT_x$ where x represents the respective aspect ratio. All other chemicals were purchased from Sigma Aldrich with purity higher than 95%.

2.2 MWCNT oxidation

The c-MWCNTs were functionalized in a microwave accelerated reaction system (mode: CEM Mars) fitted with internal temperature and pressure controls according to previously published experimental procedures.[5,6] Weighed amounts of purified MWCNTs were treated with a mixture of concentrated H_2SO_4 and HNO_3 solutions by subjecting them to microwave radiation at 140 °C for 20 min. This led to the formation of carboxylic groups on the surface leading to high aqueous dispersibility. The resulting solid was filtered through a 10 μm membrane filter, washed with water to a neutral pH and dried under vacuum at 70 °C.

The materials were characterized by scanning electron microscope (SEM), thermogravimetric analysis (TGA), and Fourier transform infrared spectroscopy (FTIR). SEM data were collected on a LEO 1530 VP scanning electron microscope equipped with an energy-dispersive X-ray analyzer. TGA was performed using a Pyris 1 TGA from Perkin-Elmer Inc from 30 °C to 900 °C under a flow of air at 10 mL min^{-1}, at a heating rate of 10 °C per min. FTIR measurements were carried out in purified KBr pellets using a Perkin-Elmer (Spectrum One) instrument.

2.3 Hydrophobicity and stability measurements

50 mg L^{-1} stock solutions of the c-MWCNTs were prepared by sonicating weighed amounts of the c-MWCNTs in MilliQ water. Various concentrations of c-MWCNTs used in this

study were then prepared by diluting the stock solution with ultrasonication. 400 mM stock solutions of sodium chloride (NaCl) and magnesium chloride ($MgCl_2$) were prepared by dissolving weighed amounts of salt in MilliQ water and dilution was carried out as needed.

Hydrophobicity of c-MWCNTs was determined in MilliQ water and in the presence of a 100 mM salt solution by measuring the UV-Visible absorbance at 500 nm before and after extraction with 1-octanol. The stability of 25 mg L^{-1} dispersions of the c-MWCNTs over a 24 hour period was determined in the presence of 25 mM solutions of sodium chloride and magnesium chloride using UV-Vis absorbance at 252 nm. The UV-Visible absorbances of 25 mg L^{-1} dispersions of the c-MWCNTs in the presence of a 25 mM salt solution were measured at time 0 hour and after standing for 24 hours. The dispersion stability index was then determined as the UV absorbance at 24 hours relative to initial UV-Visible absorbance.[23,24]

The hydrodynamic diameters of 1 mg L^{-1} dispersions of the c-MWCNTs were measured as a function of salt concentration at 25 °C using dynamic light scattering (Beckman Coulter N4 Plus submicron particle size analyzer, operated at 90° detector angle), in the presence of a 100 mM salt solution. Zeta potentials of the c-CNT dispersions were measured at a concentration of 5 mg L^{-1} at 25 °C using a Malvern Instrument (Zetasizer nano ZS90). Measurements were made in MilliQ water and in 100 mM salt environment. Data on CNT aggregation were collected using 1 mg L^{-1} dispersions of the c-MWCNTs in the presence of 100 mM electrolyte solutions. The measurements were performed for a time period ranging from 180 s to 3 h.

3. Results and discussions

3.1 Characterization

The physical characteristics of the c-MWCNTs such as outer diameter, length and aspect ratio are presented in Table 1. The c-MWCNTs studied had two length classes: short tubes with lengths of 0.5–2 μm and long tubes with lengths of 10–30 μm. Within these two length classes were five identical diameter classes (<8 nm, 10–20 nm, 20–30 nm, 30–50 nm and >50 nm).

SEM images of the c-MWCNTs are presented in Fig. 1. These show that the CNTs remained intact with minimal visible tube damage. The shorter lengths of CNTs are apparent from the SEM images of $MWCNT_{20}$, $MWCNT_{31}$, $MWCNT_{50}$, $MWCNT_{83}$ and $MWCNT_{250}$, as are the relatively smaller diameters of $MWCNT_{250}$, $MWCNT_{2608}$ and $MWCNT_{4000}$.

A representative TGA profile of the c-MWCNTs is presented in Fig. 2A. It shows weight loss in the 150 °C to 400 ° region [Fig. 2A(b)] which was absent from the purified MWCNT profile [Fig. 2A(a)]. This weight loss was attributed to the decomposition of carboxylic groups introduced through acid functionalization. The CNTs were oxidized under the same controlled reaction conditions and based on the TGA profile, the mean weight% of carboxylic groups on the CNT surface was 20.24% with a standard deviation of 3.72%. The TGA profiles of the other CNTs were similar and are not presented here for brevity.

The FTIR spectrum shown in Fig. 2B confirmed the presence of functional groups in the c-MWCNTs. The carboxylic stretching frequency occurred around 1710 cm^{-1} for all the c-MWCNTs studied indicating that they had all been oxidized. The stretching (C–O) vibration of the carboxylic group occurred around 1215 cm^{-1}. The peak around 1576 cm^{-1} was assigned to the C═C stretching of the carbon skeleton.

3.2 Hydrophobicity

1-Octanol–water partitioning was used to establish a hydro-phobicity index (HI) for the c-MWCNTs. This index was calculated based on UV-Visible absorption of the c-CNT dispersions (at 500 nm) in the original water and after 1-octanol extraction. The HI was computed as:

$$\mathrm{HI}(\%)=\frac{A_{\mathrm{o}}-A_{\mathrm{i}}}{A_{\mathrm{o}}}*100$$

where A_{o} is the UV-Visible absorbance of the c-MWCNTs before 1-octanol extraction and A_{i} is the absorbance after extraction.[23,24] After the addition of salt however some of the CNTs were extracted into the organic layer as shown in Fig. 3(a–c). This was attributed to the thinning of the electrical double layer around the c-MWCNTs by the metal ions from the salt reducing the electrostatic repulsive forces that cause the tubes to disperse in the aqueous solution and therefore causing the c-MWCNTs to settle out of the solution as shown in Fig. 3(d–f). It is apparent from Fig. 3(f) that the divalent Mg salt caused more aggregation in the c-MWCNTs than the monovalent sodium salts (Fig. 3(d and e)). Although the zeta potential values of the aqueous dispersions of the c-MWCNTs were similar, they had quite diverse HI suggesting a possible dependence on diameter and length (Fig. 4).

Fig. 4 shows the HI values of the c-MWCNTs in NaCl and $MgCl_2$ as a function of tube diameter and length. In all the c-MWCNTs studied, hydrophobicity index in deionized water was observed to be very low (Table 1), increasing with the addition of a salt. HI values for the c-MWCNTs in the presence of the divalent Mg salt were higher than those in the monovalent Na as shown in Fig. 4; this was consistent with the Schulze–Hardy rule,[9] where the critical coagulation concentration (ccc) depends upon the counterion valence z (ranges from −2 to −6).

The HI values showed no direct correlation with aspect ratios as presented in Fig. 4(a). However, it showed improved correlation with length, based on which the CNTs were categorized into two length groups (short and long). Since all the c-MWCNTs were functionalized under the same conditions, and showed similar TGA results, it is assumed that they represented similar degree of carboxylation (20.24% ± 3.72%). Therefore, the difference in the HI index was attributed to the differences in size.

The HI values were generally higher for the longer CNTs than their shorter counterparts as presented in Fig. 4(b and c). The relatively higher HI values observed in the longer c-MWCNTs were attributed to the fact that they are more prone to increased intertube attraction due to van der Waals forces and π–π interactions and are thereby more likely to form agglomerates in comparison to the shorter c-MWCNTs.[25] Dependence on CNT diameter was observed among the longer nanotubes. The higher diameter tubes probably led to the formation of denser particle aggregates because it is known that MWCNTs with larger diameters tend to comprise of more concentric tubes.[26] These bigger diameter CNTs therefore have a higher tendency to settle out of the colloidal system,[27] resulting in higher HI values. For the shorter c-MWCNTs the HI values were generally stable with increasing diameter.

3.3 Aggregation of c-MWCNTs

The particle size distribution of the c-MWCNTs in the presence of a salt as a function of diameter and length is presented in Fig. 5. The water dispersibility of c-MWCNTs originates from the negatively charged oxygen-containing groups on the CNT surface. In the aqueous phase, the electrostatic repulsive forces between negative surface charges of the oxygen-

containing groups may lead to stability of the c-MWCNTs in water. In the presence of electrolyte solutions, positively charged metal ions compressed the double layer of the dispersed nanotubes, which led to agglomeration. The longer CNTs were observed to form significantly larger aggregates than the shorter CNTs in the presence of salts [Fig. 5(b and c)] in agreement with the observed hydrophobicity index values [Fig. 4(b and c)]. This was attributed to relatively lower aspect ratios of the shorter c-MWCNTs, giving them a “stout” nature which is less prone to aggregation compared to the longer tubes with higher aspect ratios, which were more prone to intertube interactions which led to the formation of larger particle sizes. This observation was in agreement with recent data reported by Kim and co-workers on the effects of aspect ratios of CNTs on their toxicity.[28] Diameter dependence was observed among the long tubes where an increase in diameter resulted in larger particles; this was attributed to the formation of larger aggregates as a result of higher number of concentric rings. Generally, the divalent Mg salt caused higher aggregation in the c-MWCNTs resulting in larger particle sizes than the monovalent Na salts consistent with HI data [Fig. 4(b and c)].

Fig. 6 shows the zeta potential of the c-MWCNTs in electrolytic media as a function of their diameter. The zeta potential values observed agreed very well with the observed particle aggregation shown in Fig. 5. It was observed that the shorter tubes had slightly higher absolute zeta potential values than the longer tubes confirming that the longer CNTs were more prone to aggregation than their shorter counterparts. A similar dependence on CNT diameter was also observed among the long tubes, where the absolute value of zeta potential decreased with increasing diameter, which was attributed to the larger denser particle aggregates formed with increasing CNT diameter.[26] The divalent Mg salt caused a significant decrease in the zeta potential values for all the c-MWCNTs which was in agreement with the larger particle sizes observed in the Mg environment as shown in Fig. 5(b), consistent with the dependence on counterion valence as outlined by the Schulze–Hardy rule.[9]

The initial aggregation kinetics of the c-MWCNTs was investigated using time resolved dynamic light scattering. The initial rate of change in particle size (r_h) is proportional to kn_o where k is the initial aggregation rate constant and n_o is the initial concentration of the c-MWCNTs.[29] The reciprocal of the Fuchs stability ratio 1/W or the attachment efficiency α for suspensions with the same particle concentration was computed as:

$$\alpha = \frac{\left(\frac{dR_h(t)}{dt}\right)_{t\to 0}}{\left(\frac{dR_h(t)}{dt}\right)_{t\to 0,\text{fast}}}$$

where $\left(\frac{dR_h(t)}{dt}\right)_{t\to 0}$ and $\left(\frac{dR_h(t)}{dt}\right)_{t\to 0,\text{fast}}$ represent the slow and fast aggregation regimes respectively.[9,29] The attachment efficiency is a measure of the ratio of the initial slope of the aggregation profile in a given electrolyte system to the slope obtained under fast aggregation conditions. Particle aggregation in an electrolytic solution is presented as a function of time in Fig. 7(a and b). It is evident that the slope of the diameter–time profiles increased with increasing electrolyte concentration.

While a high concentration of sodium chloride was required for significant aggregation to be observed, magnesium chloride caused aggregation at concentration levels as low as 0.5 mM. The critical coagulation concentrations (ccc) of NaCl and $MgCl_2$ for aggregation of the c-MWCNTs were determined from the plot of attachment efficiencies against salt concentrations (not shown) and are plotted against the diameters of the c-MWCNTs in Fig.

7(c and d). Previously reported ccc values are significantly lower than the present data which deal with highly water dispersible MWCNTs.[9] The shorter c-MWCNTs had relatively higher ccc values under both sodium and magnesium conditions than the longer ones implying that the shorter c-MWCNTs were better stabilized under the electrolytic conditions studied. The relatively lower ccc values observed in the longer c-MWCNTs was attributed to the fact that they are more prone to increased intertube attraction due to van der Waals forces and π–π interactions and are thereby more likely to form agglomerates and bundles in comparison to the shorter c-MWCNTs. While the ccc values were generally stable with increasing tube diameter for the shorter tubes, they were observed to decrease with increasing diameter for the longer ones. This observation was in agreement with the observed HI values, particle size aggregation behavior and zeta potential values shown in Fig. 4–6 respectively. This was attributed to the phenomenon where the density of aggregates increased with increasing particle diameter[26] among the long CNTs resulting in faster settling rates and therefore lower ccc values. Significantly lower ccc values were observed in the presence of divalent Mg ions (Fig. 7(c and d)) which was also consistent with the HI, particle size and zeta potential in the presence of Mg, consistent with the Schulze–Hardy rule.[9]

3.4 Time dependent stability of the c-MWCNTs

The time dependent stability of the nanotube dispersions are presented in Fig. 8. It was observed that c-MWCNT dispersions in deionized water were stable over the 24 hour measurement period irrespective of diameter or length. In the presence of the sodium electrolytes however, the shorter tubes were generally stable with increasing tube diameter unlike the longer CNTs where stability was observed to decrease with increasing diameter, in perfect agreement with the observed HI values, particle size aggregation behavior and zeta potential values. This high-lights the greater tendency for the longer tubes to aggregate due to van der Waals intertube attraction and π–π interactions and confirms the formation of larger denser particle aggregates with increasing CNT diameter as a result of the higher number of concentric rings associated with larger diameter MWCNTs,[26] settling out of the colloidal system faster.[27] In the presence of the Mg salt all the c-MWCNTs become destabilized within 24 h, which was also in agreement with the relatively higher HI values observed in the Mg environment, consistent with the Schulze–Hardy rule[9] where ccc is said to be dependent on counterion valence.

4. Conclusions

The colloidal behaviors of c-MWCNTs of different sizes were found to be different in terms of hydrophobicity, particle size distribution, zeta potential and aggregation kinetics. The hydrophobicity indices of the c-MWCNTs showed a dependence on the length of the c-MWCNTs, where the shorter tubes showed relatively lower HI values. Zeta potential values of the c-MWCNTs showed a similar dependence on tube length where the shorter c-MWCNTs showed more negative values. This was consistent with the particle size aggregation behavior and the initial aggregation kinetics, where the longer c-MWCNTs showed significantly larger aggregates than the shorter ones, with corresponding lower ccc values. It was observed that the shorter c-MWCNTs were less prone to aggregation. The effect of CNT diameter was not very pronounced among the shorter c-MWCNTs as all the parameters investigated did not vary significantly with diameter. The colloidal behavior of the longer c-MWCNTs, however, showed a dependence on diameter where stability appeared to decrease with increasing CNT diameter. The higher diameter tubes led to the formation of denser particle aggregates due to the presence of more concentric tubes, with greater tendency to settle out of the colloidal system. There was no apparent correlation between the parameters investigated and the aspect ratio of the MWCNTs. All the c-

MWCNTs were quite stable in deionized water for the twenty four hour period studied here. Aquatic environments such as rivers, lakes, estuaries, and groundwater typically contain monovalent and divalent salts as well as other suspended and colloidal particles. Therefore an important predictor of the fate and transport of nanomaterials in these environments is the fundamental understanding of their aggregation behavior at these solution chemistries. Results from this study suggest that the dimensions of the c-MWCNTs influence their aggregation behavior under solution chemistries typical of aquatic environments.

Acknowledgments

This work was funded by the National Institute of Environmental Health Sciences (NIESH) under grant number RC2 ES018810. Any opinions, findings, and conclusions or recommendations expressed in this material are those of the author(s) and do not necessarily reflect the views of the NIESH. Partial support for this work was also provided by the Schlumberger Foundation Faculty for the Future Fellowship.

References

1. O'Connell MJ, Boul P, Ericson LM, Huffman C, Wang Y, Haroz E, Kuper C, Tour J, Ausman KD, Smalley RE. Chem. Phys. Lett. 2001; 342:265–271.
2. Zorbas V, Ortiz-Acevedo A, Dalton AB, Yoshida MM, Dieckmann GR, Draper RK, Baughman RH, Jose-Yacaman M, Musselman IH. J. Am. Chem. Soc. 2004; 126:7222–7227. [PubMed: 15186159]
3. Lin Y, Allard LF, Sun Y-P. J. Phys. Chem. B. 2004; 108:3760–3764.
4. Jeynes JCG, Mendoza E, Chow DCS, Watts PCP, McFadden J, Silva SRP. Adv Mater. 2006; 18:1598–1602.
5. Chen Y, Iqbal Z, Mitra S. Adv. Funct. Mater. 2007; 17:3946–3951.
6. Chen Y, Mitra S. J. Nanosci. Nanotechnol. 2008; 8:5770–5775. [PubMed: 19198303]
7. Yurekli K, Mitchell CA, Krishnamoorti R. J. Am. Chem. Soc. 2004; 126:9902–9903. [PubMed: 15303847]
8. Zhang J, Zou H, Qing Q, Yang Y, Li Q, Liu Z, Guo X, Du Z. J. Phys. Chem. B. 2003; 107:3712–3718.
9. Elimelech, M.; Gregory, J.; Jia, X.; Williams, R. Particle Deposition and Aggregation: Measurement, Modelling and Simulation. Butterworth-Heinemann: 1995.
10. Saleh NB, Pfefferle LD, Elimelech M. Environ. Sci. Technol. 2008; 42:7963–7969. [PubMed: 19031888]
11. Peng X, Jia J, Gong X, Luan Z, Fan B. J. Hazard. Mater. 2009; 165:1239–1242. [PubMed: 19041176]
12. Smith B, Wepasnick K, Schrote KE, Bertele AR, Ball WP, O'Melia C, Fairbrother DH. Environ. Sci. Technol. 2009; 43:819–825. [PubMed: 19245021]
13. Manivannan S, Jeong IO, Ryu JH, Lee CS, Kim KS, Jang J, Park KC. J. Mater. Sci.: Mater. Electron. 2009; 20:223–229.
14. Derjaguin B, Landau L. Prog. Surf. Sci. 1993; 43:30–59.
15. Verwey, EJW.; Overbeek, JTG. Theory of the Stability of Lyophobic Colloids. Dover Publications; 1999.
16. Karlsson HL, Gustafsson J, Cronholm P, Möller L. Toxicol. Lett. 2009; 188:112–118. [PubMed: 19446243]
17. Pan Y, Neuss S, Leifert A, Fischler M, Wen F, Simon U, Schmid G, Brandau W, Jahnen-Dechent W. Small. 2007; 3:1941–1949. [PubMed: 17963284]
18. Napierska D, Thomassen LCJ, Rabolli V, Lison D, Gonzalez L, Kirsch-Volders M, Martens JA, Hoet PH. Small. 2009; 5:846–853. [PubMed: 19288475]
19. Yuan H, Gao F, Zhang Z, Miao L, Yu R, Zhao H, Lan M. J. Health Sci. 2010; 56:632–640.
20. Javey A, Guo J, Paulsson M, Wang Q, Mann D, Lundstrom M, Dai H. Phys. Rev. Lett. 2004; 92:106804. [PubMed: 15089227]
21. Liu F, Zhang X, Cheng J, Tu J, Kong F, Huang W, Chen C. Carbon. 2003; 41:2527–2532.

22. Wang XX, Wang JN, Chang H, Zhang YF. Adv. Funct. Mater. 2007; 17:3613–3618.
23. Addo Ntim S, Sae-Khow O, Witzmann FA, Mitra S. J. Colloid Interface Sci. 2011; 355:383–388. [PubMed: 21236442]
24. Wang X, Xia T, Addo Ntim S, Ji Z, George S, Meng H, Zhang H, Castranova V, Mitra S, Nel AE. ACS Nano. 2010; 4:7241–7252. [PubMed: 21067152]
25. Heister E, Lamprecht C, Neves V, Tilmaciu C, Datas L, Flahaut E, Soula B, Hinterdorfer P, Coley HM, Silva SR, McFadden J. ACS Nano. 2010; 4:2615–2626. [PubMed: 20380453]
26. Chiodarelli N, Richard O, Bender H, Heyns M, De Gendt S, Groeseneken G, Vereecken PM. Carbon. 2012; 50:1748–1752.
27. Crowder TM, Rosati JA, Schroeter JD, Hickey AJ, Martonen TB. Pharm. Res. 2002; 19:239–245. [PubMed: 11934228]
28. Kim J, Lee K, Lee Y, Cho H, Kim K, Choi K, Lee S, Song K, Kang C, Yu I. Arch. Toxicol. 2011; 85:775–786. [PubMed: 20617304]
29. Schudel M, Behrens SH, Holthoff H, Kretzschmar R, Borkovec M. J. Colloid Interface Sci. 1997; 196:241–253. [PubMed: 9792750]

Environmental impact

Aquatic environments such as rivers, lakes, estuaries, and groundwater typically contain monovalent and divalent salts as well as other suspended and colloidal particles. Therefore an important predictor of the fate and transport of nanomaterials in these environments is the fundamental understanding of their aggregation behavior at these solution chemistries. Results from this study suggest that the dimensions of the c-MWCNTs influence their aggregation behavior under solution chemistries typical of aquatic environments, thus giving insights into the potential influence of CNT dimension on their fate and transport.

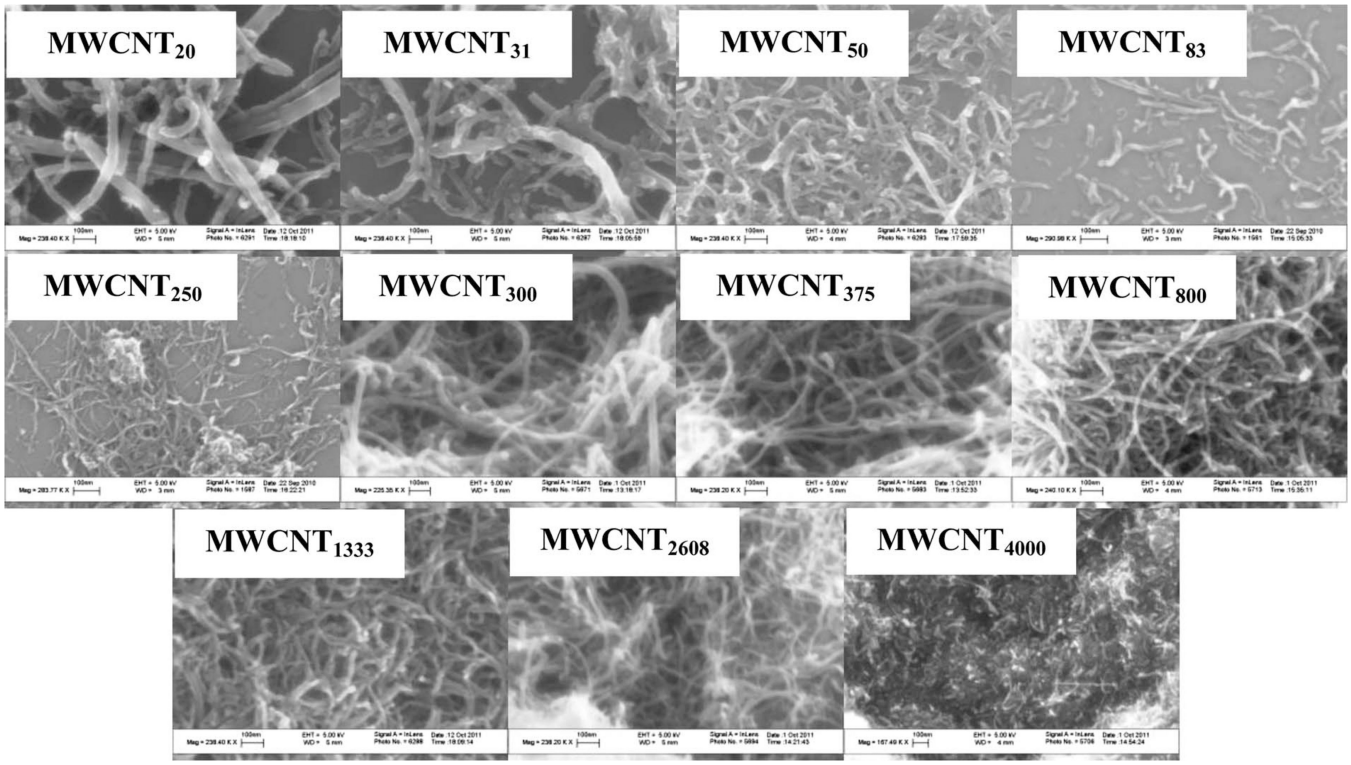

Fig. 1.
Scanning electron microscope images of the c-MWCNTs.

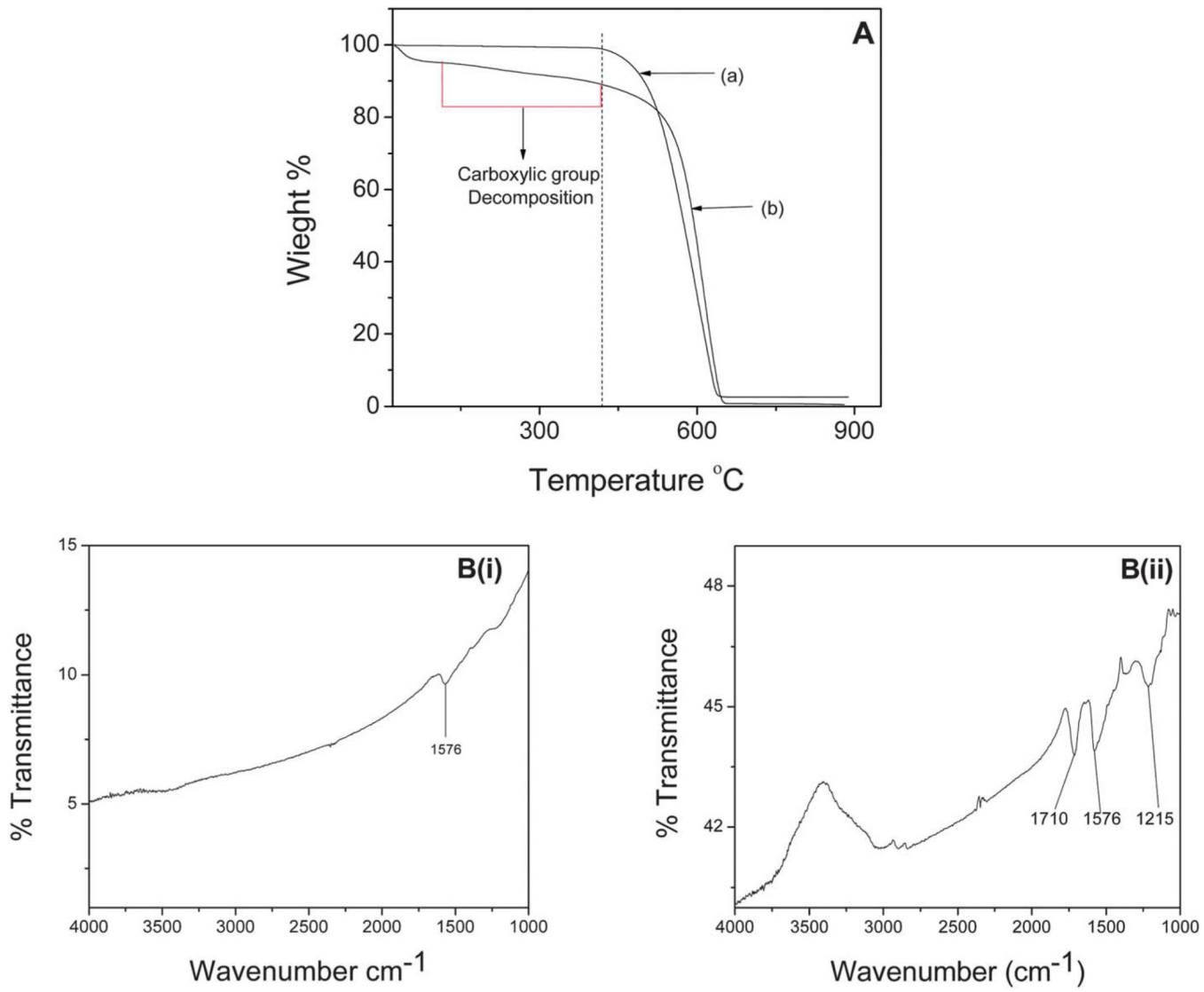

Fig. 2.

A (a) TGA data for purified MWCNTs, (b) representative TGA profile of the c-MWCNTs showing MWCNT83, (c); B (i) FTIR spectra of purified MWCNTs and (ii) representative FTIR spectra of the c-MWCNTs showing $MWCNT_{250}$.

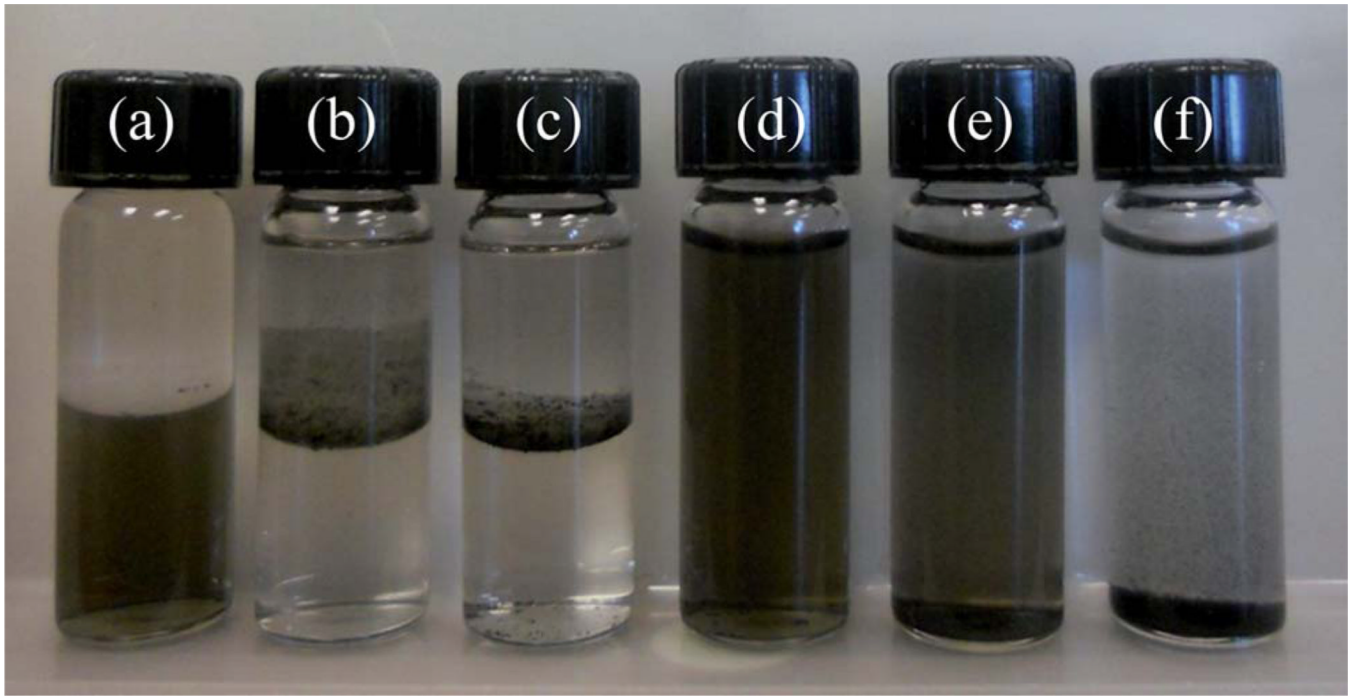

Fig. 3.
1-Octanol extraction of c-MWCNTs in (a) DI water, (b) 25 mM NaCl, and (c) 25 mM $MgCl_2$, and particle aggregation in the presence of (d) DI water, (e) 25 mM NaCl, and (f) 25 mM $MgCl_2$.

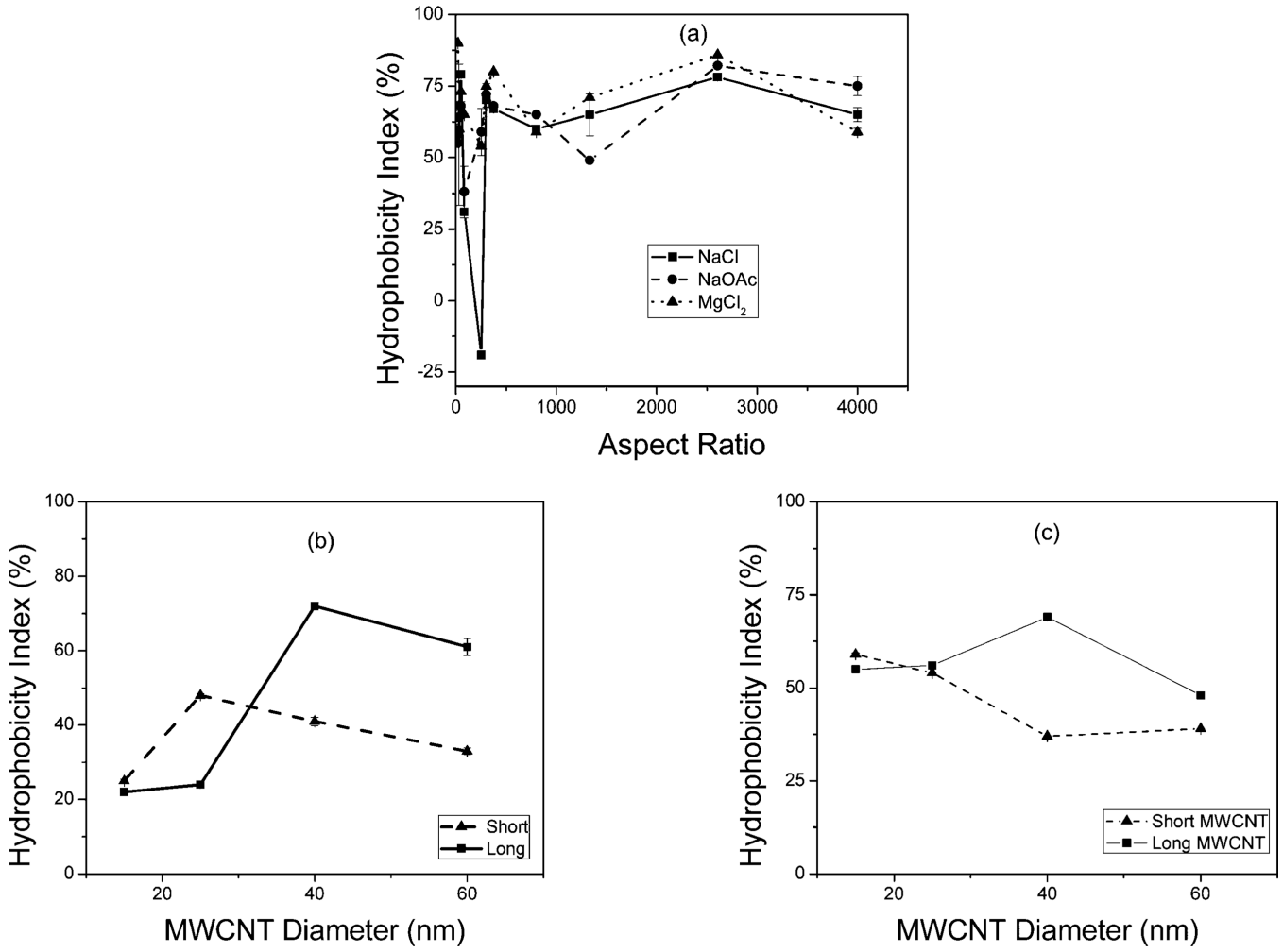

Fig. 4.

Hydrophobicity index of the c-MWCNT as a function of (a) aspect ratio and as a function of diameter in the presence of 100 mM (b) NaCl and (c) $MgCl_2$.

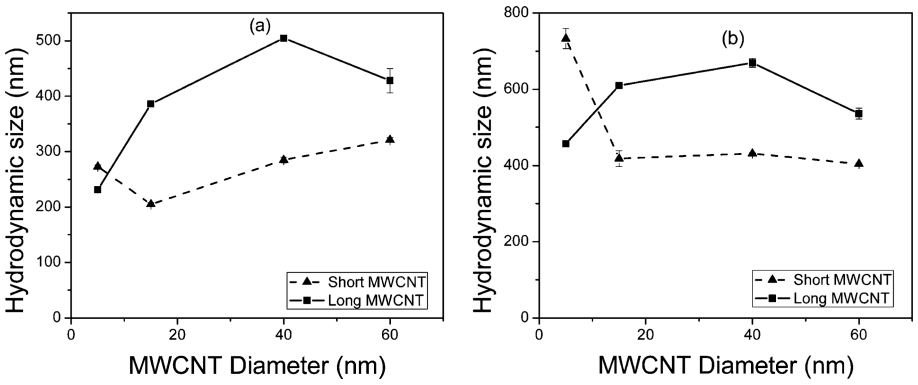

Fig. 5.

Particle size distribution in a 100 mM electrolyte solution as a function of tube diameter for the c-MWCNTs in the presence of (a) NaCl and (b) $MgCl_2$.

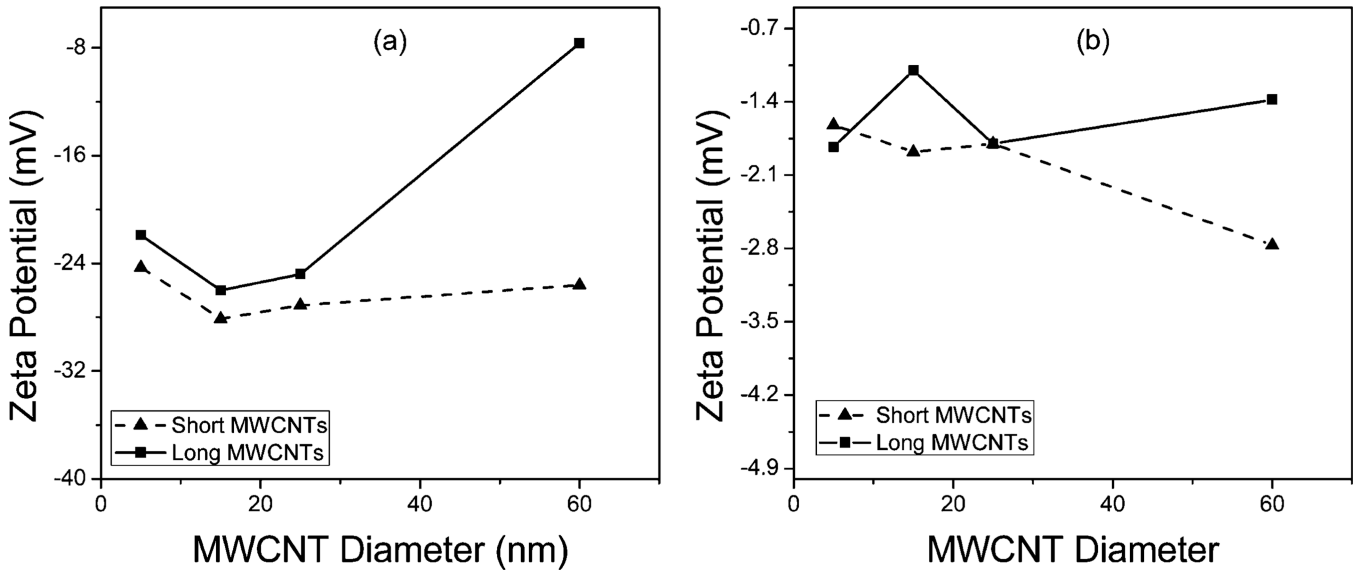

Fig. 6.

Zeta potential as a function of diameter for the c-MWCNTs in the presence of (a) NaCl and (b) $MgCl_2$.

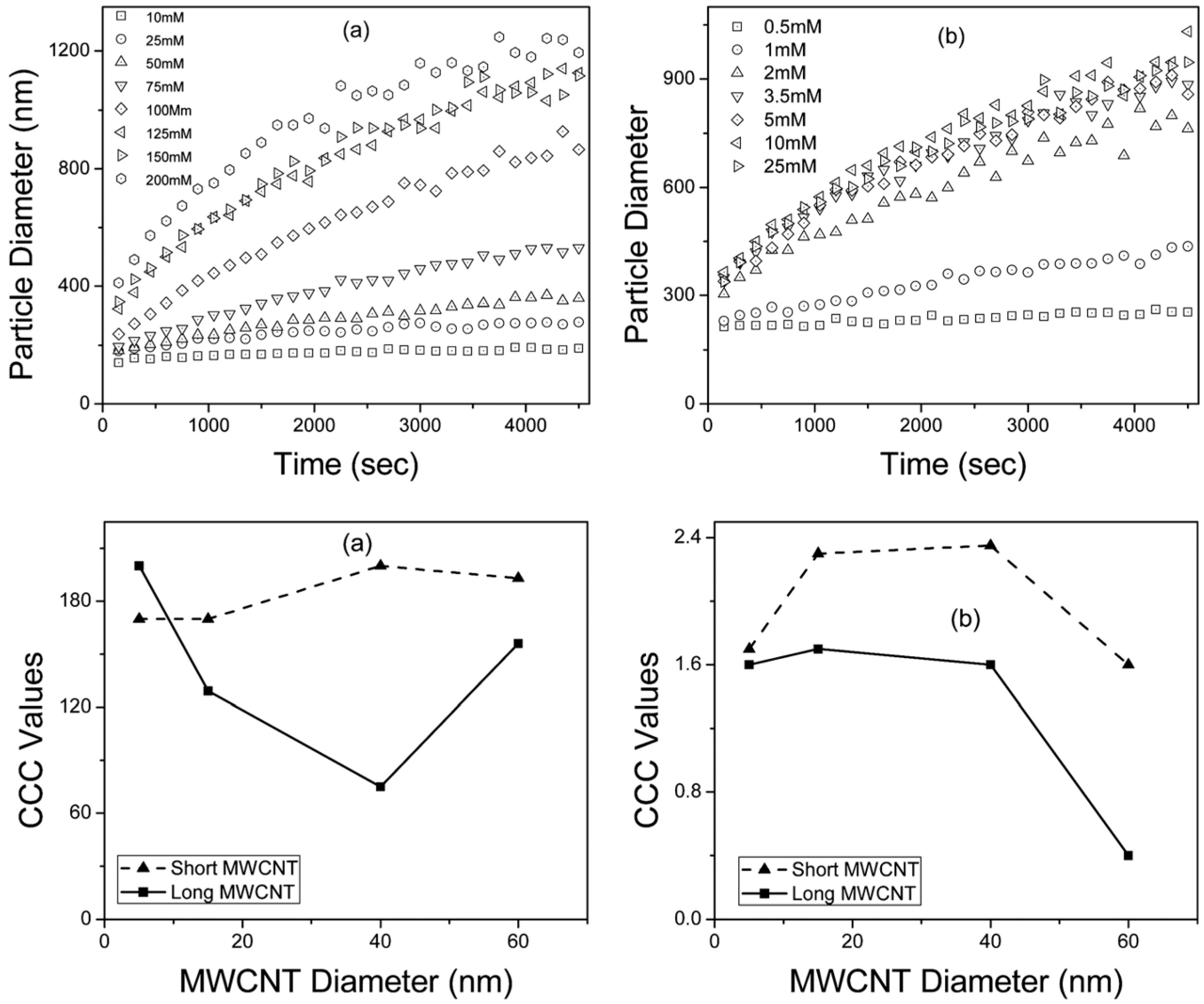

Fig. 7.

Particle size as a function of time in the presence of (a) NaCl and (b) $MgCl_2$ and attachment efficiency as a function of c-MWCNT diameter in the presence of (c) NaCl and (d) $MgCl_2$.

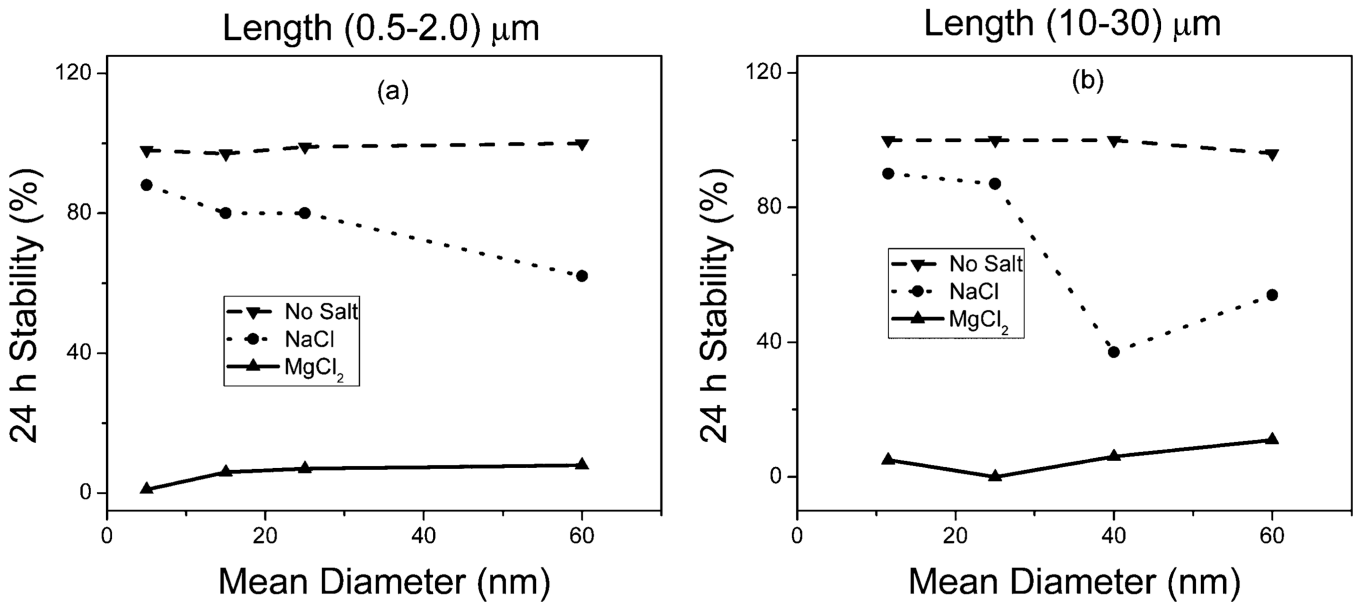

Fig. 8.
Colloidal stability as a function of c-MWCNT diameter for (a) short c-MWCNTs and (b) long c-MWCNTs.

Table 1

Physical characterization of the c-MWCNTs

CNT ID	OD (nm)	Length (μm)	Aspect ratio	HI index in DI water (%)
$MWCNT_{20}$	>50	0.5–2	20	−22
$MWCNT_{31}$	30–50	0.5–2	31	3
$MWCNT_{50}$	20–30	0.5–2	50	−6
$MWCNT_{83}$	10–20	0.5–2	83	−3
$MWCNT_{250}$	<8	0.5–2	250	−23
$MWCNT_{300}$	>50	10–20	300	−6
$MWCNT_{375}$	30–50	10–20	375	−1
$MWCNT_{800}$	20–30	10–30	800	−4
$MWCNT_{1333}$	10–20	10–30	1333	−8
$MWCNT_{2608}$	8–15	10–50	2608	−7
$MWCNT_{4000}$	<8	10–30	4000	−6